

Reconstruction of missing energy in events with two photons at the ATLAS detector in Large Hadron Collider

K G Tomiwa^{1*}, Xifeng Ruan¹, Shell-may Liao¹, Bruce Mellado¹

¹ School of Physics, University of the Witwatersrand, Johannesburg 2050, South Africa

E-mail: kehinde.gbenga.tomiwa@cern.ch

Abstract. The missing transverse momentum in the ATLAS experiment is defined as the momentum imbalance in the plane transverse to the beam axis. That is the resultant of the negative sum of all the particles that are detected. A precise estimation of the missing transverse energy is essential for many physics studies at the LHC, such as Higgs boson estimated in the diphoton decay channel, as well as for searches of physics beyond the Standard Model. The reconstruction of missing energy is sensitive to the presence of additional collisions, usually referred to as pile-up. A new method is being proposed to reduce the effect of pileup events in ATLAS experiment. This article describes the performance of missing energy in respect to the improvement of vertex methods in ATLAS experiment.

1. Introduction

Missing transverse energy (E_T^{miss}) is very important to many physics analysis in the Large Hadron Collider (LHC). The missing transverse energy is used in the Higgs boson searches and search for physics Beyond the Standard Model (BSM) like the evidence of supersymmetry or hidden sector particles like the dark matter particles. Unlike most Standard Model particles the dark matter particles and neutrinos do not leave traces inside particle physics detectors, because of the non-interacting nature of these particles with detector material we can only infer their presence through missing transverse energy in the detector.

The E_T^{miss} is transverse momentum imbalance created by the detector and well-measured objects in an event [1]. Previous studies have shown that the reconstruction and measurement of the E_T^{miss} are greatly affected by pileup interaction from other proton-proton collision vertices in the same bunch crossing event [2], this in turns leads to what is known as fake E_T^{miss} . The same vertex method is introduced and its performance in suppressing fake E_T^{miss} is studied. This method is used in searches in the decay channel of Higgs to two photons in association with E_T^{miss} [3]. The corresponding phenomenology is described in Ref [4].

2. ATLAS Detector

The ATLAS detector is one of the particle detectors in the LHC, the detector is built around one of the interacting points along the LHC ring. It is a multipurpose system of particle detector used in measuring missing transverse energy, jet energy, hadrons taus, and muons. The detector

Table 1. Samples used for the background processes relevant in this analysis. The $V\gamma$ and $V\gamma\gamma$ are leptonic decay including Z to neutrinos. using full simulation (Full Sim) and Fast simulation (AFII) procedures

Process	Num. Events	Generation	Simulation
ggF, $h \rightarrow \gamma\gamma$ 125 GeV	95000	PowhegPythia8EvtGen AZNLOCTEQ6L1	Full Sim
Zh , $h \rightarrow \gamma\gamma$ 125 GeV	49800	Pythia8EvtGen A14NNPDF23LO	Full Sim
$h \rightarrow \gamma\gamma + 3$ Jets	106010000	Sherpa CT10	AFII
$V\gamma$ ($V = Z, W^\pm$)	4991400	Sherpa CT10	Full Sim
$V\gamma$ ($V = Z, W^\pm$)	6982000	Sherpa CT10	Full Sim
$V\gamma\gamma$ ($V = Z, W^\pm$)	29800	Sherpa CT10	Full Sim
$V\gamma\gamma$ ($V = Z, W^\pm$)	38000	Sherpa CT10	Full Sim
mH275mx60	5000	PowhegPythia8EvtGen AZNLOCTEQ6L1	Full Sim

is composed of three main systems namely the inner detector (ID), the hadronic calorimeter and the muon spectrometer, the three systems are arranged in a barrel-plus-endcaps [5].

The inner detector covers the pseudorapidity range of $\eta < 2.5$, it has three layers (silicon pixel detector, silicon microstrip detector, and transition radiation tracker). The ID is used for precise vertex measurement, extra tracking of particles and particle identification. There are two types calorimeters in the ATLAS detector, the liquid argon (LAr) sampling electromagnetic calorimeter which is situated outside next to the hadronic calorimeter (TileCal), it covers region of $|\eta| < 3.2$ and the steel scintillator tile calorimeter (TileCal) covering the range of $|\eta| < 1.7$. The muon spectrometer (MS) is the outer most part of the ATLAS detector, the MS is used in the reconstruction of the muon. Each subsystem of the ATLAS detector has different functionality, they are combined to in measuring physics processes.

3. Monte Carlo samples used

The samples used for performance checks are listed in table 1. These samples are classified into two categories, based on whether the samples physics processes will lead to real or fake E_T^{miss} . The gluon-gluon fusion (ggF) and $\gamma\gamma$ are Higgs signal and background samples respectively, these samples have no process that leads to E_T^{miss} , hence E_T^{miss} estimated in this samples are regarded as fake E_T^{miss} . The other samples in the list are: Zh , $V\gamma$, $V\gamma\gamma$ and MH275mx260 (BSM sample with decay dark matter particle) are particles with real E_T^{miss} , the E_T^{miss} is as a result of either dark matter particle or decay to neutrinos.

4. Reconstruction of E_T^{miss}

E_T^{miss} is an imbalance in the sum of energy of all particles in the transvers plane of the detector, it is reconstructed using the energy deposited in the calorimeter and muon spectrometer. The E_T^{miss} components are calculated by:

$$E_{x(y)}^{\text{miss}} = E_{x(y)}^{\text{miss,calo}} + E_{x(y)}^{\text{miss,}\mu} \quad (1)$$

The calorimeter term in Equation 1 is calculated based on reconstructed physics objects (electrons, photons, taus, jets and muons) associated with cells, cells which are not associated with physics objects are tagged $E_{x(y)}^{\text{miss,CellOut}}$. The $E_{x(y)}^{\text{miss,calo}}$ term is given by:

$$E_{x(y)}^{\text{miss,calo}} = E_{x(y)}^{\text{miss,calo},e} + E_{x(y)}^{\text{miss,calo},\gamma} + E_{x(y)}^{\text{miss,calo},\tau} + E_{x(y)}^{\text{miss,calo,jets}} + E_{x(y)}^{\text{miss,calo},\mu} + E_{x(y)}^{\text{miss,CellOut}} \quad (2)$$

each term in Equation 2 is calculated from the negative sum of the calibrated cell energies corresponding to objects as follows:

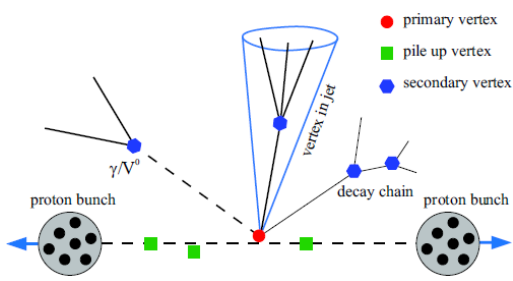


Figure 1. Vertex in the ATLAS detector [6]

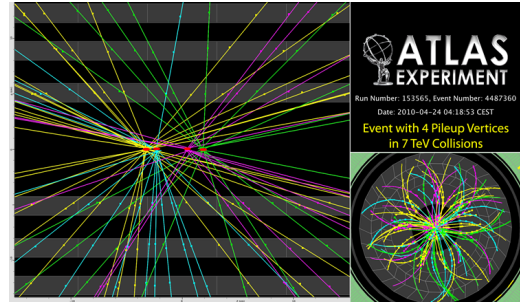


Figure 2. Vertices in the ATLAS detector [6]

$$E_x^{miss,term} = - \sum_{i=1}^{N_{cell}} E_i \sin \theta_i \cos \phi_i, \quad E_y^{miss,term} = - \sum_{i=1}^{N_{cell}} E_i \sin \theta_i \cos \phi_i \quad (3)$$

The muon term in Equation 1 is calculated from the momenta of muon reconstructed with $|\eta| < 2.7$ as follows:

$$E_{x(y)}^{miss,\mu} = - \sum_{muons} P_{x(y)}^{\mu} \quad (4)$$

E_T^{miss} and its angle ϕ^{miss} are calculated by:

$$E_T^{miss} = \sqrt{(E_x^{miss})^2 + (E_y^{miss})^2}, \quad \phi^{miss} = \arctan(E_y^{miss}, E_x^{miss}) \quad (5)$$

5. Vertex of interaction in ATLAS detector

Figures 1 and 2 show some typical vertices during proton-proton collision in the ATLAS detector, only one of these vertices is the vertex of interaction for physics process (primary vertex). Most analysis in ATLAS used the method called the hardest scatter (HS) vertex method in reconstructing or identifying the primary vertex, the hardest vertex method identifies the primary vertex as the vertex with the highest scalar sum square of transvers momentum out of all vertex ($\sum (p_T^{track})^2$).

This method is not effective for the analysis with photons like the $H \rightarrow \gamma\gamma + E_T^{miss}$, hence another method called photon pointing method was developed [2]. Since photons tracks are seen in the calorimeter (except for converted photons), this method employed a neural network algorithm (K-nearest neighbor algorithm) in pointing two photons tracks from the calorimeter to the inner detector, so the point of interception is identified as the primary vertex.

6. Pile-up in ATLAS detector and pile-up suppression methods

Pile-up vertices are the other vertices due to additional collisions accompanying the HS collision. The jet term of the E_T^{miss} algorithm uses the jet vertex tagger (JVT) index to suppress pile-up [2]. A cut is placed on jet $p_T > 60$ GeV, $|\eta| > 2.4$ and $|JVT| > 0.59$.

From Fig. 3 we see the JVT cut is not 100% efficient in the suppression of pileup, about 40% of events cannot be distinguished as either from PU or HS collision. This introduce fake missing E_T^{miss} . in addition to this Fig. 4 illustrates the scenario which can lead to fake E_T^{miss} , when the JVT cut rejects a jet object in an event due to cut efficiency, the E_T^{miss} algorithm sometimes identified this rejected object as missing energy. This is the motivation behind the development of the same vertex method.

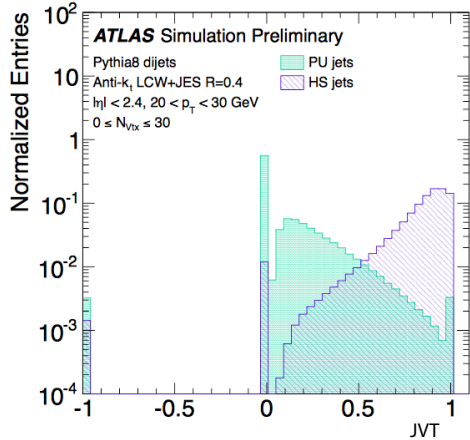


Figure 3. JVT PU and HS jets [6]

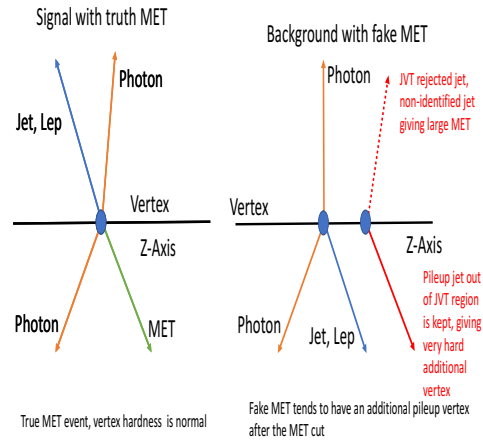


Figure 4. Same vertex method

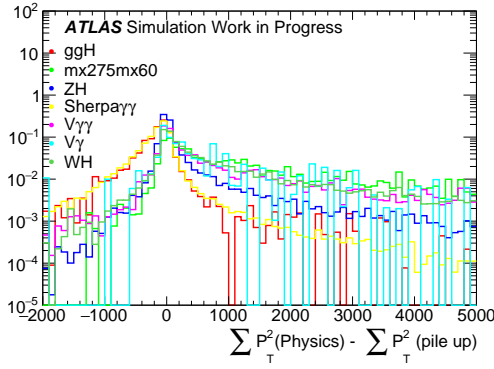


Figure 5. Difference between hardest vertex method and photon pointing methods

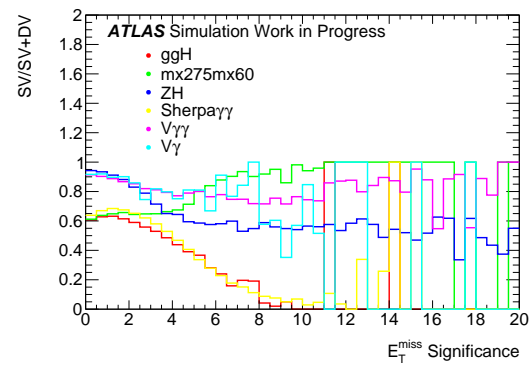


Figure 6. Fraction of event that pass E_T^{miss} significance cut

7. Same vertex method

The same vertex method tries to reduce or distinguish between background and signal events by comparing the consistency between the two vertex reconstruction methods, the same vertex method places an additional requirement on event selection, the vertex selected by the hardest scattered vertex (HS) must be same as the one selected by the photon pointing (PP) vertex selection method. This is implemented by requiring the $\sum(p_T^{\text{track}})^2(\text{Physics}) - \sum(p_T^{\text{track}})^2(\text{Pile-up})$ to be larger than 0. The same vertex method is used in addition to the selection using E_T^{miss} and E_T^{miss} significance (defined as $E_T^{\text{miss}} / E_T^{\text{miss}} \text{resolution}$).

Figure 5 shows the distribution of $\sum(p_T^{\text{track}})^2(\text{Physics}) - \sum(p_T^{\text{track}})^2(\text{Pile-up})$ for different samples, the region [-5000,0] is region of fake E_T^{miss} , the samples with fake E_T^{miss} have a higher number of events in this region as compared with the samples with real E_T^{miss} . An opposite observation is seen in the other region of the distribution [0, 5000] as the samples with real E_T^{miss} have a higher number of events. This trend shows that $\sum(p_T^{\text{track}})^2(\text{Physics}) - \sum(p_T^{\text{track}})^2(\text{Pile-up})$ is effective in identifying an isolated event with fake E_T^{miss} .

Figure 6 shows the fraction of events that passes the same vertex selection against the inclusive selection in E_T^{miss} significance bins. Again we see the same vertex method is able to separate

samples with fake E_T^{miss} and real E_T^{miss} , a veto on E_T^{miss} significance greater 3.0 will significantly reduce background events.

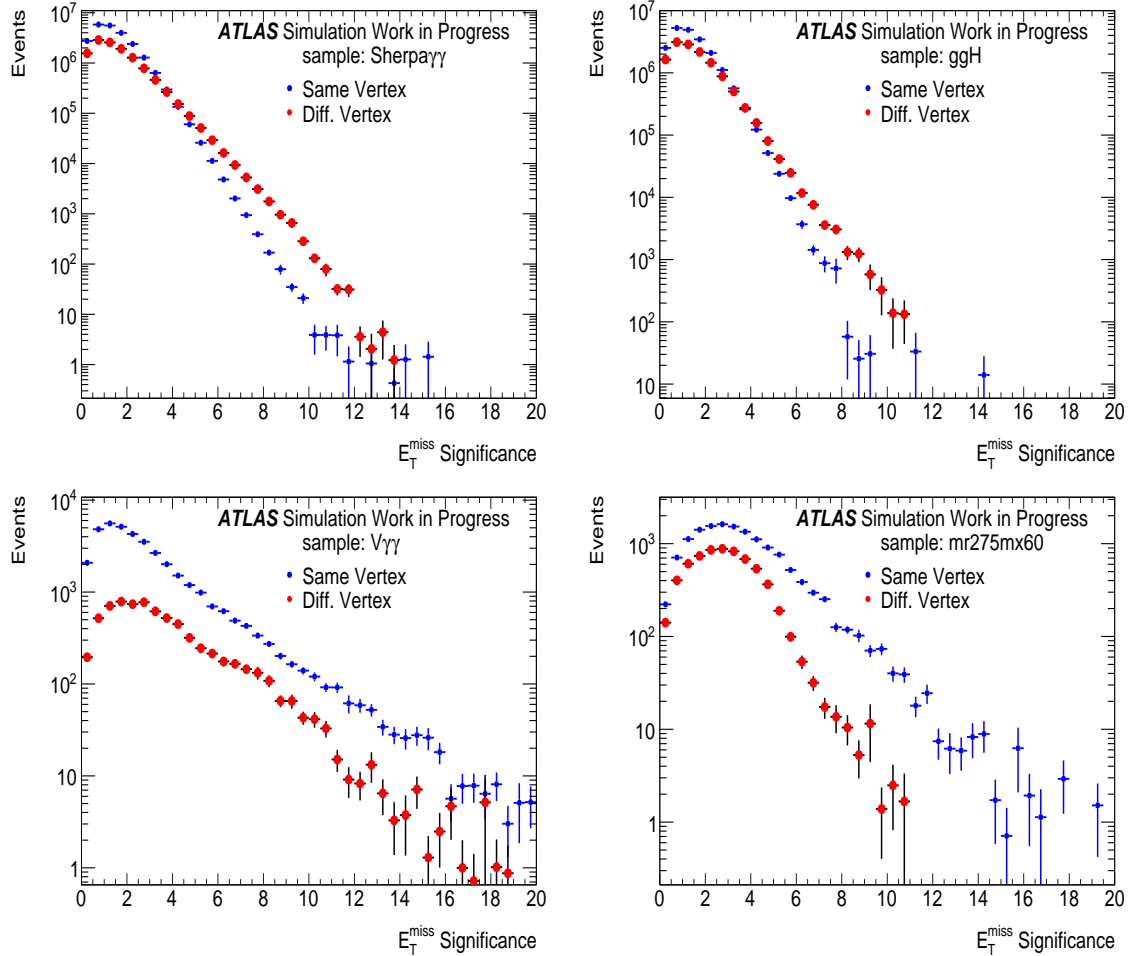


Figure 7. Events in same vertex and different vertex for different sample

7.1. Performance of same vertex method

Figure 7 shows the performance of selecting events with the same vertex method as compared with selecting events without the same vertex method (different vertex) for ggF, $h \rightarrow \gamma\gamma + 3\text{jets}$, $V\gamma$ and $V\gamma\gamma$. ggF and $h \rightarrow \gamma\gamma + 3\text{jets}$ are samples with fake E_T^{miss} and they have comparable event distributions in the same vertex and different vertex phase space, this is because of the contribution from fake E_T^{miss} arising from the JVF cut and Pile-up contribution. This implies events with fake E_T^{miss} can be rejected without losing much efficiency in the analysis. On the other hand, events with different vertex selection are much lower than the events with same vertex selection for $V\gamma$ and $V\gamma\gamma$ (samples with real E_T^{miss}) as expected.

Figures 8 and 9 show the mass spectrum of Higgs decay to two photons in the Higgs signal side-band (background). Figures 8 is the side band without any requirement on same vertex method and Figures 9 is the side-band with a requirement on same vertex method after a E_T^{miss} significance > 5.5 . A significant reduction (about 60%) in signal side-band events is seen by comparing the two distributions.

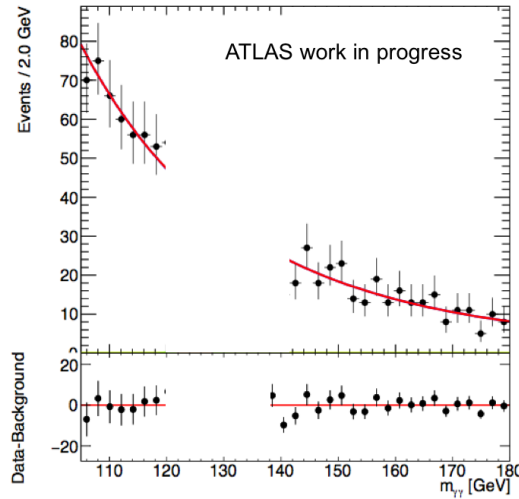


Figure 8. Blinded-data Sideband without same vertex cut

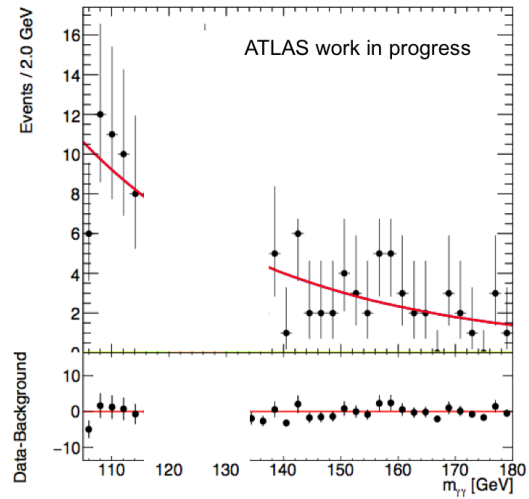


Figure 9. Blinded-data Sideband with same vertex cut

8. Conclusions

This paper has presented a new method of suppressing background events in the search for dark matter particles in ATLAS detector. The missing transverse energy is important to the search for new physics and $H \rightarrow \gamma\gamma + E_T^{miss}$ process in particular. However, the reconstruction missing transverse is sensitive to pile-up event from jets, miss-identification of photons or jets events which may lead to fake E_T^{miss} . To mitigate the effect of this error a study on the vertex selection was done and it was observed that background events and fake E_T^{miss} events can be significantly reduced by requiring same vertex from the Photon pointing and Hardest scattered method of vertex reconstruction. From Figures 8 and 9 about 60% of background events were reduced by using the same vertex method, this method has been validated by the ATLAS performance group. The same vertex method has been used in the search for dark matter in association with a Higgs boson decaying to two photons [3].

References

- [1] Hrynevich A (ATLAS Collaboration) 2017 ATLAS jet and missing energy reconstruction, calibration and performance in LHC Run-2 Tech. Rep. ATL-PHYS-PROC-2017-045. 06 CERN Geneva URL <https://cds.cern.ch/record/2263777>
- [2] Aaboud M *et al.* (ATLAS Collaboration) 2014 Tagging and suppression of pileup jets with the ATLAS detector Tech. Rep. ATLAS-CONF-2014-018 CERN Geneva URL <https://cds.cern.ch/record/1700870>
- [3] Aaboud M *et al.* (ATLAS Collaboration) 2017 (*Preprint* 1706.03948)
- [4] von Buddenbrock S, Chakrabarty N, Cornell A S, Kar D, Kumar M, Mandal T, Mellado B, Mukhopadhyaya B, Reed R G and Ruan X 2016 *Eur. Phys. J.* **C76** 580 (*Preprint* 1606.01674)
- [5] Aaboud M *et al.* (ATLAS Collaboration) 2009 (*Preprint* 0901.0512)
- [6] Aaboud M *et al.* (ATLAS Collaboration) 2016 *Eur. Phys. J. C* **77** 332. 52 p